



Site characterization report at the seismic station IV.TRTR- Tortoreto (TE)

Report di caratterizzazione di sito presso la stazione sismica IV.TRTR - Tortoreto (TE)

| | |
|---|---------------------|
| Working Group Geology: Deborah Di Naccio Geophysics: Giuseppe Di Giulio, Maurizio Vassallo, Luca Minarelli | Date: December 2020 |
| Subject: Final report illustrating the site characterization for seismic station IV.TRTR | |

**INDEX**

| | |
|--|-------|
| <i>Introduction</i> | 3 |
| A. Geological setting | 4-10 |
| 1. Topographic and geological information | 4 |
| 2. Geological map | 6 |
| 3. Lithotechnical map | 7 |
| 4. Survey map | 8 |
| 5. Geological model | 9 |
| 5.1 General description | 9 |
| 5.2 Geological section | 9 |
| 5.3 Subsoil model | 10 |
| B. Vs profile | 11-25 |
| 1. Preface | 12 |
| 2. Geophysical Investigation | 14 |
| 2.1 H/V noise spectral ratio of temporary stations | 15 |
| 2.2 H/V noise spectral ratio using data of IV.TRTR | 18 |
| 2.3 Array analysis | 19 |
| 2.3.1 Active data from the 1D array of geophones | 19 |
| 2.3.2 Passive data from the 1D array of geophones | 20 |
| 2.3.3 Passive data from the 2D array of seismic stations | 20 |
| 2.3.4 Selection of the dispersion curve | 23 |
| 3. Seismic Velocity model | 24 |
| 4. Conclusion | 26 |
| <i>References</i> | 27 |
| <i>Disclaimer and limits of use of information</i> | 29 |
| <i>Summary Reports</i> | 30 |



INTRODUCTION

In this report we present the geological setting and the geophysical measurements and results obtained in the framework of the 2019-2021 agreement between INGV and DPC, called *Allegato B2: Obiettivo 1 - TASK 2: Caratterizzazione siti accelerometrici (Responsabili: G. Cultrera, F. Pacor)* for the site characterization of station IV.TRTR (Tortoreto, Teramo).

Location and coordinates are reported in Table 1.

Table 1.

| CODE | NAME | LAT [°] | LON [°] | ELEVATION [m] |
|---------|---|-----------|-----------|---------------|
| IV.TRTR | Tortoreto (TR) | 42.80810* | 13.91380* | 160* |
| ADDRESS | Località Tortoreto Alta, Stadio delle Fontanelle, Via dello Sport, 64018 Tortoreto Teramo TE, Italy | | | |

* Coordinates from ITACA (Nov. 2020)



A. Geological setting

A1. TOPOGRAPHIC AND GEOLOGICAL INFORMATION

Topographic information related to the site is reported in Table 2. Table 3 summarizes all available geological maps from literature for geological analyses.

Table 2.

| Topography | Description | Topography Class | Morphology Class | EC8 Class |
|------------|--|------------------|------------------|-----------|
| | Flat surfaces, isolated slope and reliefs with slope $i \leq 15^\circ$ | T1 | P* | B |

*Reference table from ITACA (Nov. 2019)

Table 3.

| Geological map | Source | Scale |
|----------------|--|-----------|
| IV.TRTR | Geological map of Italy sheets 133-134 (Ascoli Piceno-Giulianova) | 1:100.000 |
| IV.TRTR | Carta Geologica d'Abruzzo (Vezzani & Ghisetti, 1998). | 1:100.000 |
| IV.TRTR | Carta Geologica-Tecnica per la Microzonazione Sismica di Livello 1, Regione Abruzzo, comune di Tortoreto(TE) (January, 2014) | 1:5.000 |

In Table 4 Geological and Lithotechnical Units (according to Seismic Microzonation classification; Technical Commission SM, 2015) are described and are concerned to maps of following chapters. The term “original” means the result comes from a preexisting cartography (Table 3); the term



“deduced” means the result comes from an interpretation of preexisting cartography according to the nomenclature of corresponding cartography.

Table 4

| GEOLOGICAL UNITS | | LITHOTECHNICAL UNITS | |
|---|-------------------------|----------------------|--|
| “Geological Map of Italy, scale 1:100:000” (Sheets 133-134; Ascoli Piceno-Giulianova) <i>original</i> | | (Mzs) <i>deduced</i> | |
| code | description | code | description |
| col | colluvial deposits | GMec | gravel, mixture of gravel, sand and silt |
| col | colluvial deposits | Mlec | inorganic silt, fine grained silty or clayey sand, clayey silt with low plasticity |
| Q1c | conglomerates | GR | Cemented granular rocks. |
| Q1b | stratified yellow sands | GRS | Layered cemented granular rocks. |



A2. GEOLOGICAL MAP

In Figure 1 Geological Map is reported in a 1kmx1Km square around the station.

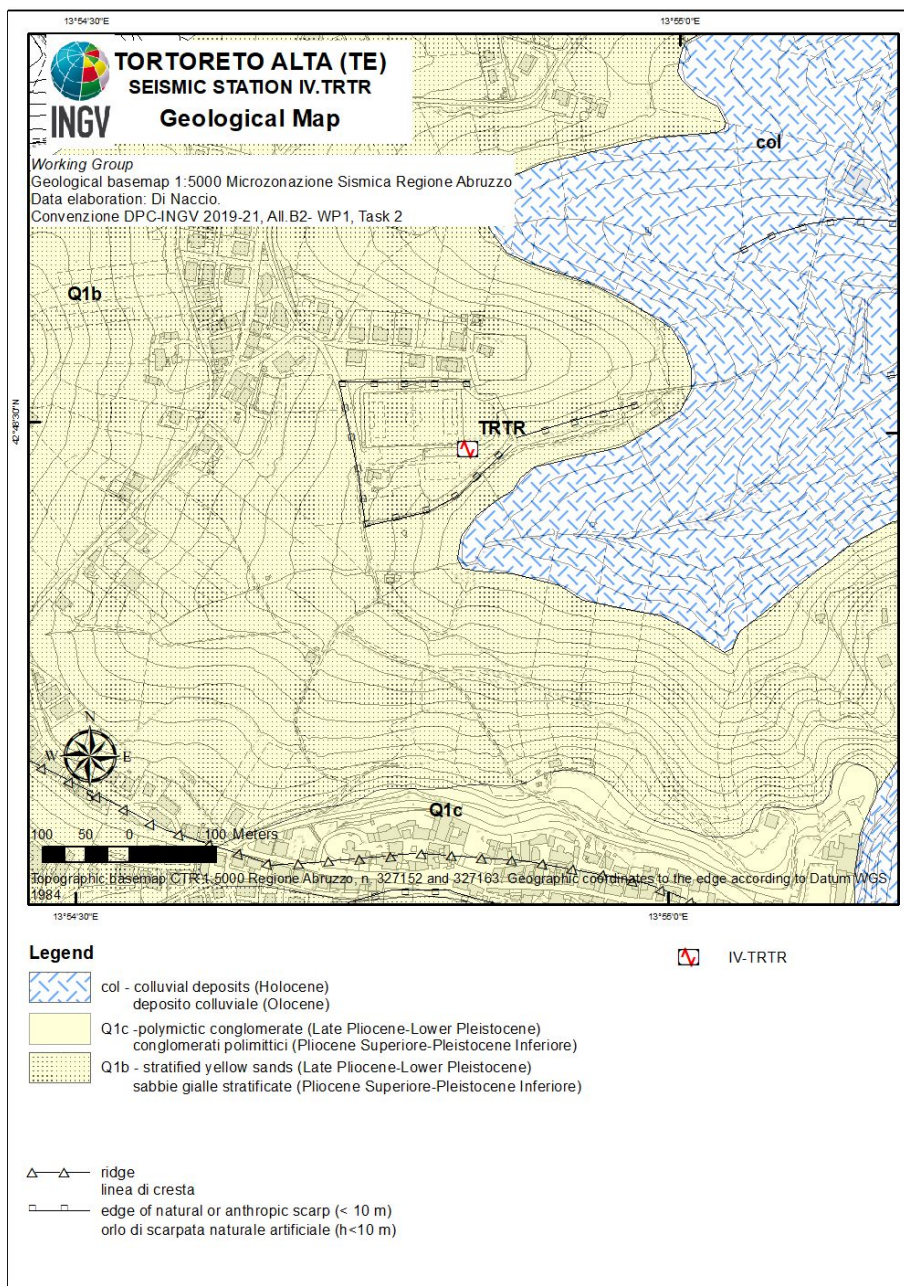


Figure 1. Geological map of seismic station IV.TRTR. Scale 1:5.000. Geological units come from the "Geological Map of Italy, scale 1:100:000 (Sheet 133-134; Ascoli Piceno-Giulianova)".



A3. LITHOTECHNICAL MAP

In Figure 2 Lithotechnical Map is reported in a 1kmx1Km square around the station.

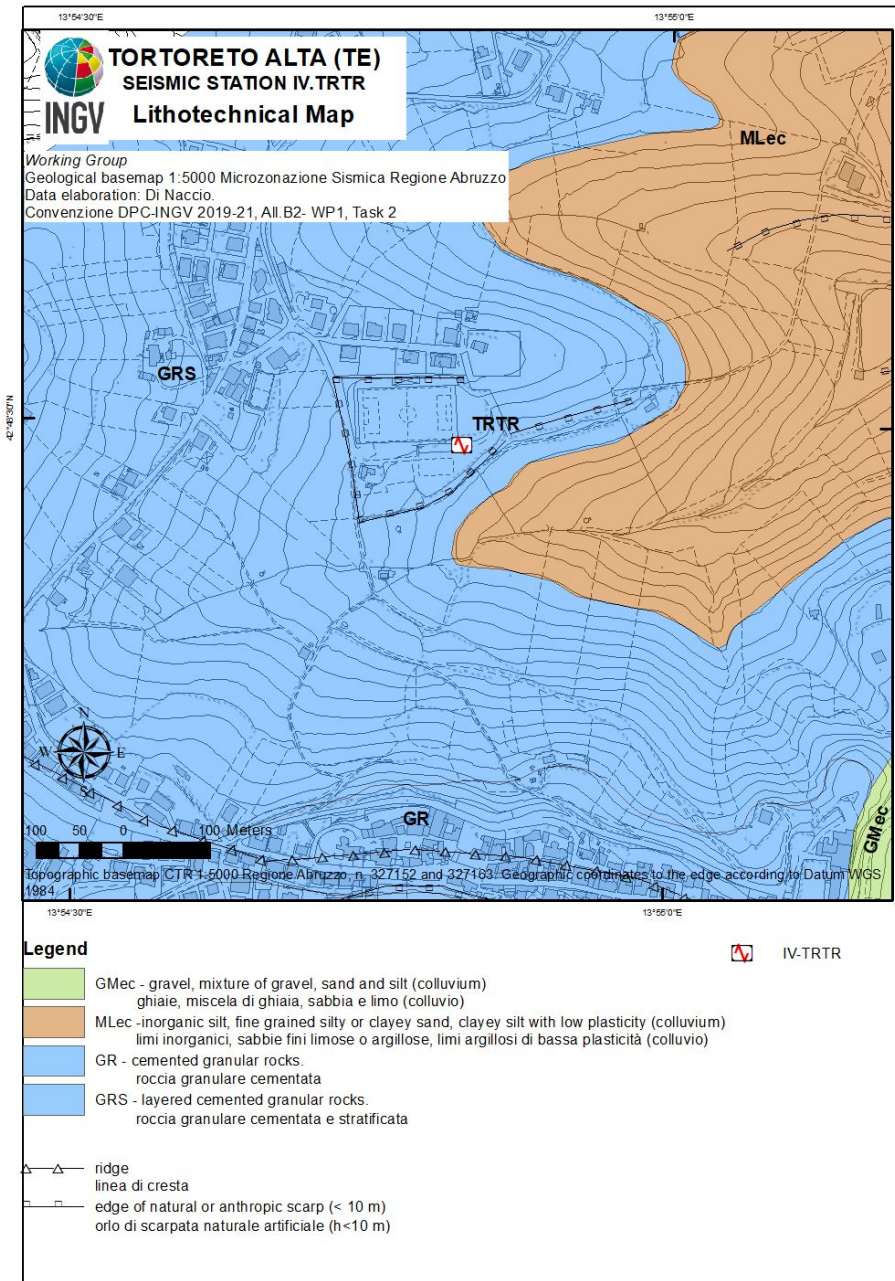


Figure 2: Lithotechnical map of the seismic station IV.TRTR. Scale 1:5.000. The lithotechnical units are deduced from the "Carta Geologica-Tecnica per la Microzonazione Sismica di Livello 1, Regione Abruzzo, comune di Tortoreto(TE), scale 1:5:000 (2014) and assigned according to the nomenclature of Seismic Microzonation (Technical Commission SM, 2015).



A4. SURVEY MAP

Figure 3 shows the Survey Map reporting investigations and geophysical surveys conducted by INGV Working Group.

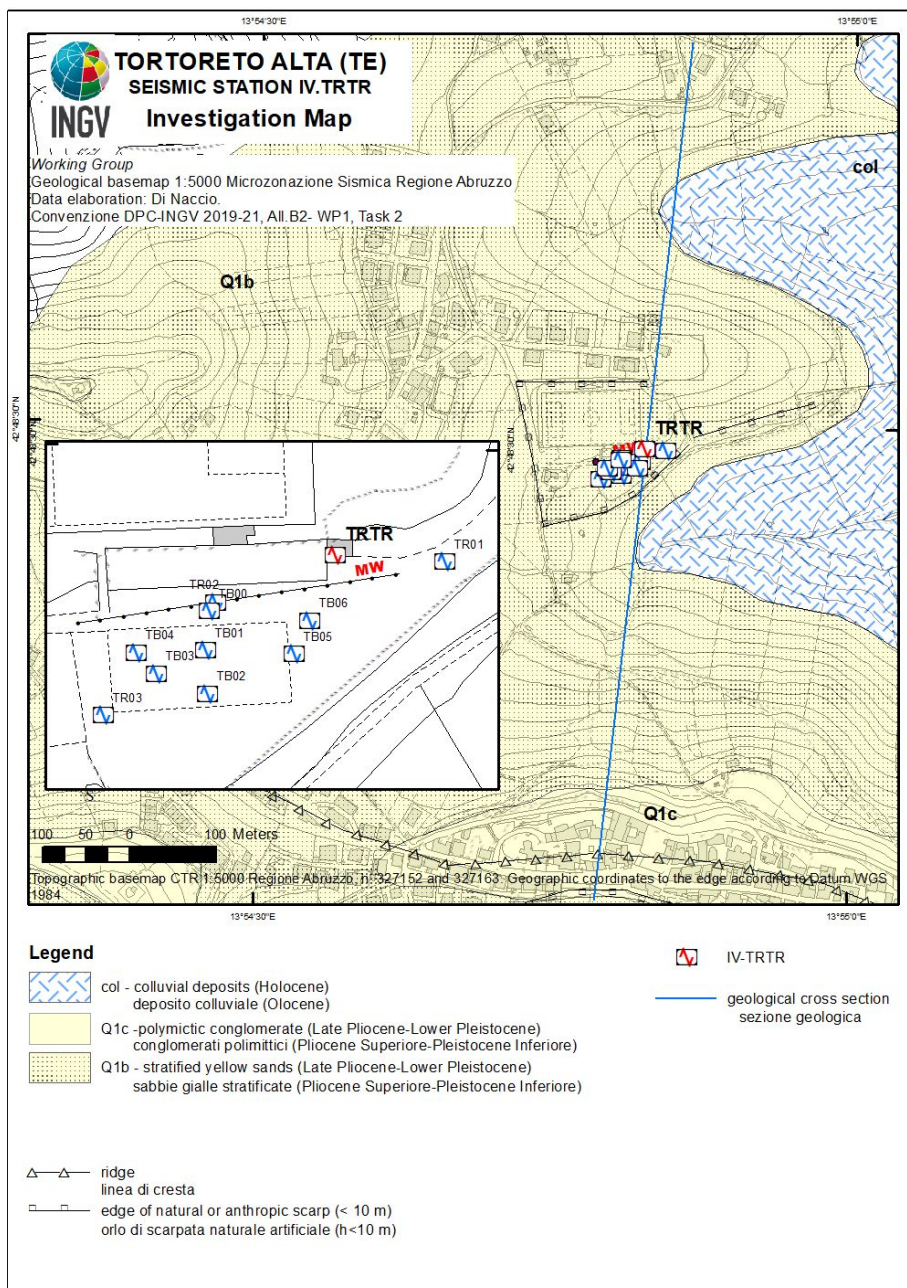


Figure 3: Map of the surveys in the surroundings of the station IV.TRTR. Scale 1:5.000. The box at the left contains a zoom of the area with the detail of the geophysical survey conducted by INGV Working Group for the seismic characterization of the site (see part B. "Vs profile" in this report).



A5. GEOLOGICAL MODEL

5.1 General description

The seismic station is installed in the Marche-Abruzzi sector of the Periadriatic basin developing at the front of the Apennine chain. The basin records the latest evolutionary stages of the compressional tectonic and regional uplift of the Apennine thrust and fold belt since Neogene-Quaternary time.

Meso-Cenozoic carbonate successions crop out in the Montagna dei Fiori-Montagnone ridge to the west and in the Gran Sasso, Morrone and the Maiella Mountains to the south.

To the east of thrust fronts, foredeep siliciclastic sequences, progressively younger moving toward the Adriatic sea, crop out. They correspond to the Upper Messinian turbidites of the Laga basin, to the Lower Pliocene sandstones and clays of the Cellino basin, and to the Middle Pliocene-Pleistocene post-orogenic sequences deposited within the Periadriatic basin.

In the studied area the geological bedrock consists of a sequence of marine clayey-sandy-conglomeratic deposits (Upper Pliocene-Lower Pleistocene) in a gently NE-dipping monoclinal setting. Alluvial, slope, colluvial and landslide superficial deposits cover the bedrock.

The seismic station is at an altitude of ~ 160 m above sea level and it is located in a local plain. The bedrock is represented by the yellow sands (Q1b in Figure 1). Conglomerates (Q1c in Figure 1) overlay the Q1b unit and generally crops out at the top of hills (Figure 1). Downward, the sequence consists mostly of silt and clay strata not outcropping in the studied area and indicated as blue-grey clays (Q1a) in the Geological map of Italy (sheet 133). The bedrock is covered by colluvial deposits of ~ 3-20m-thick.

5.2 Geological Section

The geological cross section and the subsoil model (Figures 3 and 4) accompanying geological survey map provide an interpretation of the third dimension. It is based on the extrapolation of surface data with pre-existing geological and structural studies, geophysical investigations and the determined seismic velocities profiles (see part B of this report) as well as data from other subsurface sources.

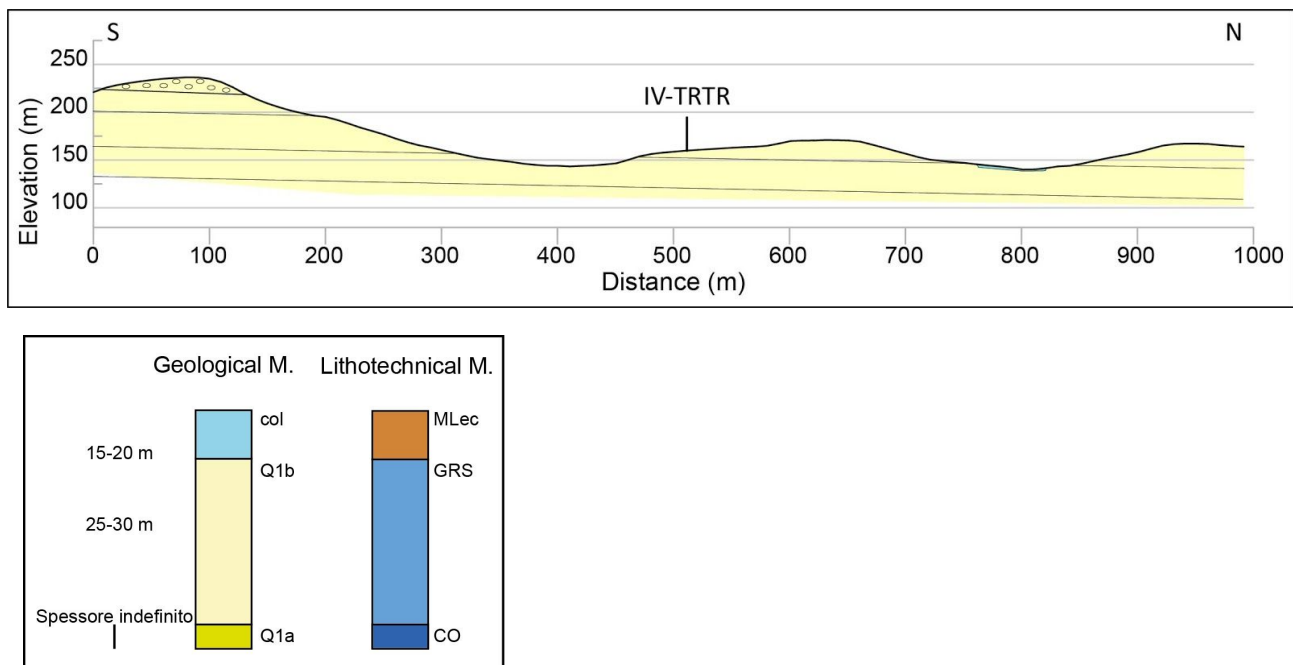


Figure 4. Top: Geological section across IV.TRTR seismic station (see Figure 3 for location); Bottom: subsoil model for the site. See Figure 1 and 2 for symbology.

5.3 Subsoil model

The lithotechnical units considered representative of the site around the IV-TRTR-seismic station (Figures 1-2 and Table 4) are the following:

GRS: layered granular rocks consisting of yellow sands. A thin layer of colluvium-eluvium (MLec) mainly consisting of fine grained deposits can cover the GRS deposit whereas its bottom can overlay cohesive clays (Q1a, in the Italian Geological Map) as recognized by geophysical modeling (part B of this report).



B. Vs profile

| | |
|--|----|
| B1. PREFACE | 12 |
| B2. GEOPHYSICAL INVESTIGATIONS | 14 |
| 2.1 H/V noise spectral ratio of temporary stations | 15 |
| 2.2 H/V noise spectral ratio using data of IV.TRTR | 18 |
| 2.3 Array analysis | 19 |
| 2.3.1 Active data from the 1D array of geophone | 19 |
| 2.3.2 Passive data from the 1D array of geophone | 20 |
| 2.3.3 Passive data from the 2D array of seismic stations | 20 |
| 2.3.4 Selection of the dispersion curve | 23 |
| B3. SEISMIC VELOCITY MODEL | 24 |
| B4. CONCLUSIONS | 26 |
| <i>References</i> | 27 |
| <i>Disclaimer and limits of use of information</i> | 29 |
| Summary Reports | 30 |



B1. PREFACE

In this section, the geophysical surveys carried out to characterize IV.TRTR station are presented. We performed a MASW experiment with an active source by using 72 vertical geophones installed in linear configuration. In combination with the MASW survey, we installed 10 seismic stations near IV.TRTR for ambient seismic noise recordings that were used for computation of the H/V curve (horizontal-to-vertical noise spectral ratio). Data records of IV.TRTR were also extracted and analyzed in terms of H/V noise ratio. Using surface-wave frequency-wavenumber analysis, we provide results in terms of resonant peaks of the H/V curves, and dispersion curves that were inverted to obtain shear-wave velocity (V_s) profiles for the studied area. The inverted models are suitable for determination of the average V_s velocity in the uppermost 30 m (V_{s30}) and assigning then the soil class category as prescribed by building codes (EC8, NC8 or NC18). The software of analysis was Geopsy (www.geopsy.org; Wathélet et al. 2020). The date of the geophysical survey was 15 September 2020. A preliminary survey to check the field logistic was conducted on 24th of June 2020, with two further noise measurements. Both days of the experiments were sunny and without wind. The first survey of 24th June 2020 helped us to decide the position of the extensive geophysical investigations carried out the 15th September 2020. The position of the cabinet hosting IV.TRTR is attached at the concrete bleacher of a football/rugby field (called “Stadio delle Fontanelle”; see Figs. 1 and 2). The difference in elevation between the housing of IV.TRTR and the football field is about 10 m, and the ground morphology indicates that the football field was subjected to an anthropic leveling especially in the eastern part. To investigate the homogeneity of the seismic response between the football field and its base (where IV.TRTR is ubicated), during the preliminary survey we performed two simultaneous noise measurements using 2 stations equipped with triaxial geophones (4.5 Hz natural frequency, Terrabot stations by Sara Electronics). These two stations (T106 and T105; Fig. 1) were installed at the level of the football field and at its base (i.e. same level of IV.TRTR), and the time-length of each noise recording was about 2 hours. The H/V noise spectral ratio at the uppermost T106 site shows a magnification in the frequency band 3-10 Hz which is absent at the bottom T105 site. Because the H/V spectral ratios using data records of IV.TRTR (see ???)



are in good agreement with the H/V ratios of T105, we decided to perform the extensive geophysical investigation of 15 September 2020 not in the football field, but along the driveway and on the concrete square at the base of the blatcher (i.e. at the same level of the IV.TRTR position; Fig.s 1 and 2).

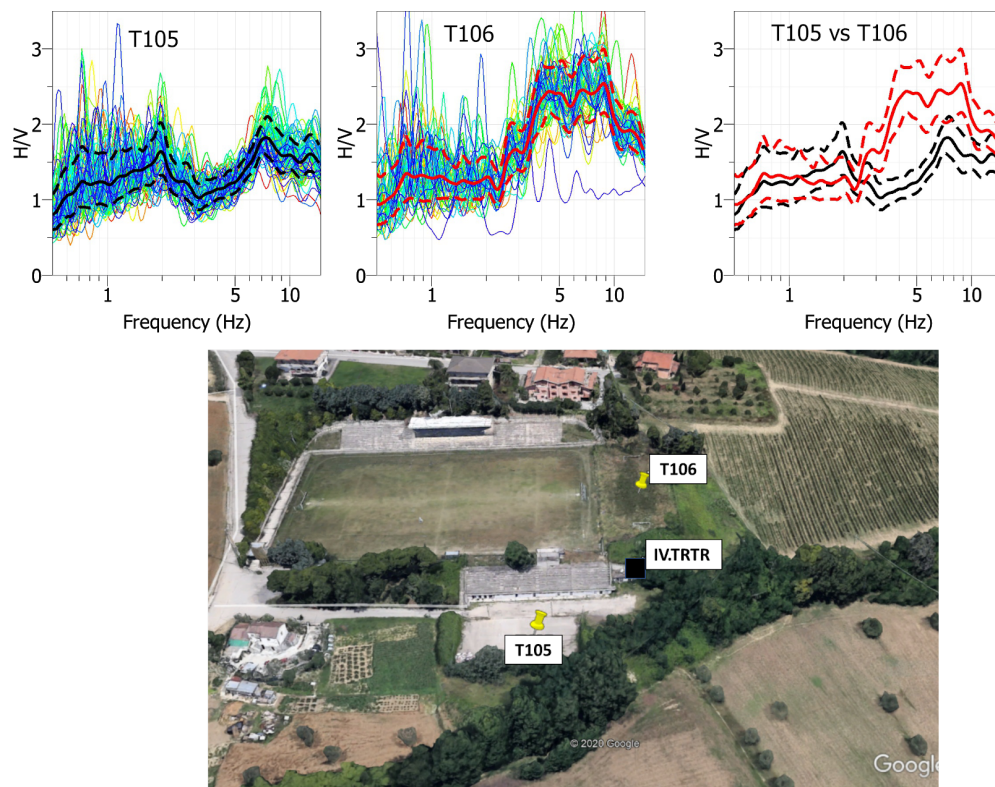


Figure 1. Preliminary geophysical survey (24th June 2020). The IV.TRTR station is indicated as black square in the google map. The yellow marks show the positions of the 2 temporary seismic stations deployed for seismic noise acquisition (T105 and T106, Terrabot equipment). On the top panel the H/V noise spectral ratios of T105 and T106 are compared.



Figure 2. Pictures showing the driveway (left); the cabinet housing IV.TRTR and the bleacher of the stadium (middle); the driveway and the concrete square are seen from the level of the uppermost football field (right).



B2. GEOPHYSICAL INVESTIGATION

We now describe the extensive geophysical survey of 15th September 2002. The map of Figure 3 shows the position of: IV.TRTR station, the MASW line of geophones (yellow line), and the temporary seismic stations deployed in the target area (yellow and red markers of Fig. 3). The linear MASW array was composed of 72 vertical geophones equipped with vertical sensors (4.5 Hz natural frequency) equally spaced of 1 m for a total length of 71 m. Noise measurements were performed by 7 stations equipped with triaxial geophones (4.5 Hz natural frequency, Terrabot stations by Sara Electronics; the TB stations in Fig. 3 in red colour) and 3 stations composed of a Reftek130 digitizer with Lennartz-5s sensor (TR01, TR02 and TR03 stations in Fig. 3 in yellow color). The time-length of each noise measurement was about 3 hours.

TR02 and TB00 were collocated at the same position in proximity of the middle of the MASW line. Unfortunately the TR03 station was subjected to a malfunctioning of the vertical component and was not used in the analysis.

Figure 4 shows some details of the installation of the MASW line and seismic sensors. The vertical geophones were placed using ad hoc plastic bases and it was not possible to bury the sensors (with the exception of TR01). The position of the noise measurements and of geophones was taken by a GPS RTK Leica antenna, with a precision of the order of a few centimeters. All the geophysical measurements shown in Figures 3 and 4 were recorded the 15th September of 2020 (it was a sunny day, no wind).

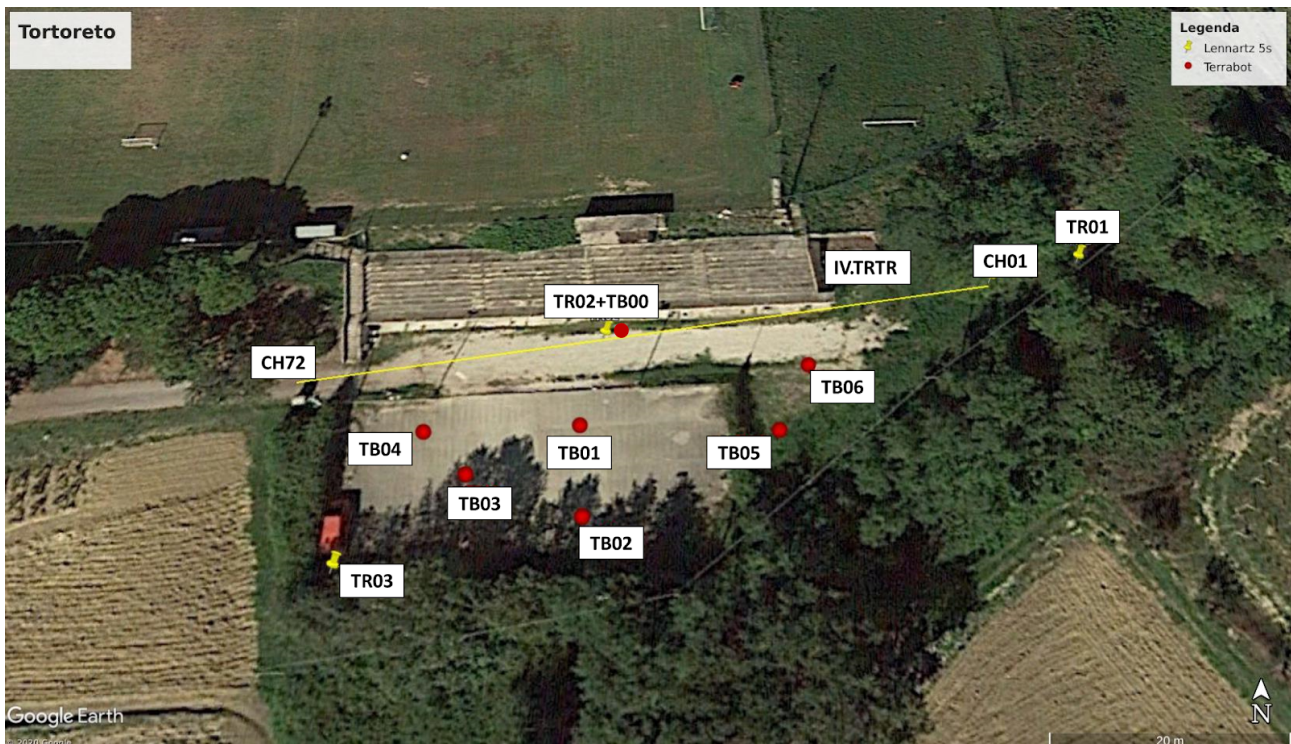


Figure 3. Google map of the geophysical surveys for the IV.TRTR station. The yellow line shows the linear MASW array of 72 vertical geophones (CH01 and CH72 indicate the first and last geophone of the line). The yellow and red marks show the positions of the 10 temporary seismic stations deployed for seismic noise acquisition (TB and red flag for Terrabot seismometer; TB and yellow flag for Lennartz 5s velocimeter). TR02 and TB00 were collocated to the same position.



Figure 4. Deployment of MASW line and seismic stations. The last two pictures show the TR01 station (Lennartz 5s velocimeter with a Reftek130 digitizer) and the TB03 station (Terrabot).

2.1 H/V noise spectral ratio of temporary stations

Figure 5 shows the H/V curves obtained from the temporary seismic stations. Details of computations are reported in the summary reports. The results of Fig. 5 indicate a good agreement in terms of H/V shapes for all the stations, with a main peak in the H/V curves at



very low frequencies, i.e. below 0.5 Hz. Of course the more reliable sites for such frequencies are the ones equipped with the Lennartz 5s (eigen-frequency of 0.2 Hz), even if the Terrabot stations provide in the studied environment similar H/V shapes in Figure 5. This low-frequency peak, at least at 0.2 Hz, is likely related to the presence of a very deep seismic contrast (order of 1 km) or to the Adriatic sea, which is about 2 km far in the easternmost direction. Other weak H/V peaks occur at 2 Hz and 6 Hz, with a moderate amplitude level which is below 2. TR01, the most eastern station, is the only site where the peak starting from about 6 Hz is most pronounced. The directional H/V curves are also shown in Figure 5, and the color scale is in some way biased by the high-amplitude peak at 0.2 Hz. For this reason, the same directional H/V curves are also presented in Figure 6 starting from a different lower frequency (0.5 Hz) and selecting an uniform logarithmic color scale. Figure 6 shows that the weak H/V peak as 2 Hz is almost isotropic, i.e. not depending by horizontal direction. Figure 7 shows the comparison of the H/V curves at all measurements points.

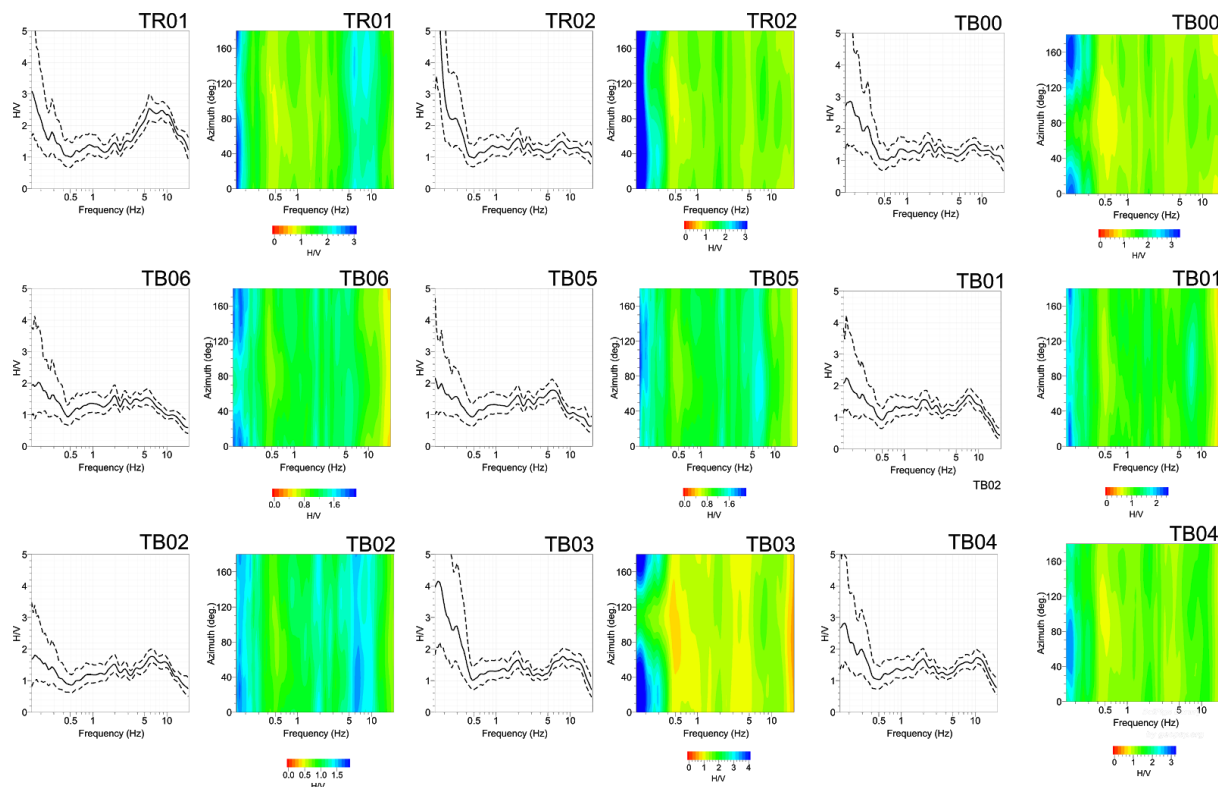


Figure 5. H/V noise spectral ratios. The seismic stations recorded ambient vibrations for about three hours (TR the Lennartz 5s velocimeters, TB indicates Terrabot instruments). TR03 was not considered in the analysis for a malfunctioning on the vertical component. TR02 and TB00 were colocated at the same position. The directional H/V curves use a linear colour scale, which is scaled for each site to a maximum value of H/V amplitude.

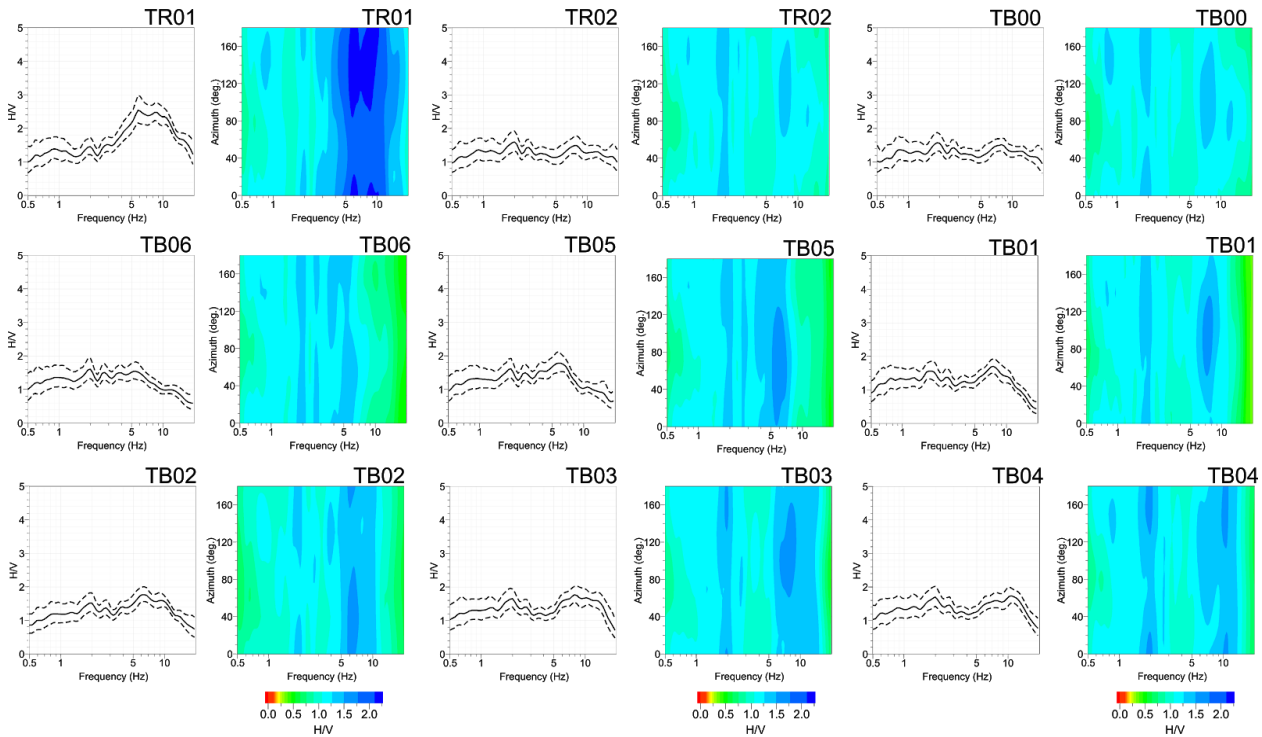


Figure 6. As Figure 5 but selecting the lower limit of the frequency axes at 0.5 Hz, and using a logarithmic color scale in the directional H/V curves (same colour scale for all the plots).

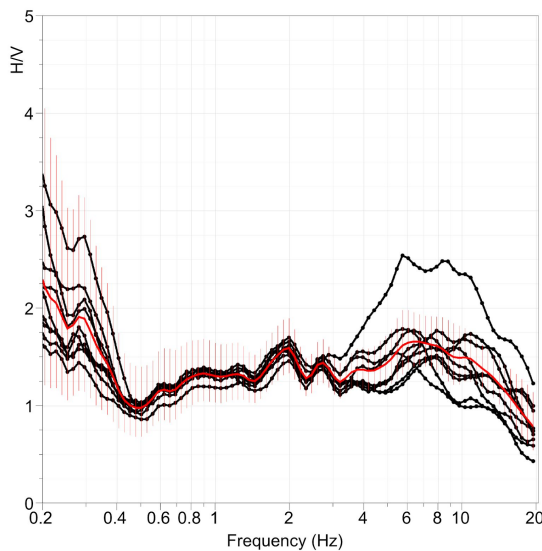


Figure 7. The mean H/V curves of all measurements are overlaid. Their average and standard deviation are shown by the red one.



2.2 H/V noise spectral ratio using data of IV.TRTR

To further investigate the H/V noise spectral ratios at IV.TRTR, we extracted continuous two-months data for four years recorded by this station (on channel HH which corresponds to a Nanometrics Trillium 40 s; data extracted from 1 january to 28 February for years 2016, 2017, 2018 and 2019). We performed the H/V computation averaging the H/V curve day by day. The results of Figure 8 confirm essentially the results of the temporary measurements of our geophysical survey, with the presence of a predominant peak in the low-frequency range below 0.2 Hz (average amplitude value around 2.2). Additional very weak peaks occur between 1 and 10 Hz, and in particular the peak at 1 Hz emerging from the H/V time-analysis is more defined with respect to the one shown in Fig. 7 by the temporary stations. The H/V signature of the several peaks in the range 1-10 Hz is very consistent over time, but due to their low-amplitude values are not considered as resonant frequencies in the next analysis.

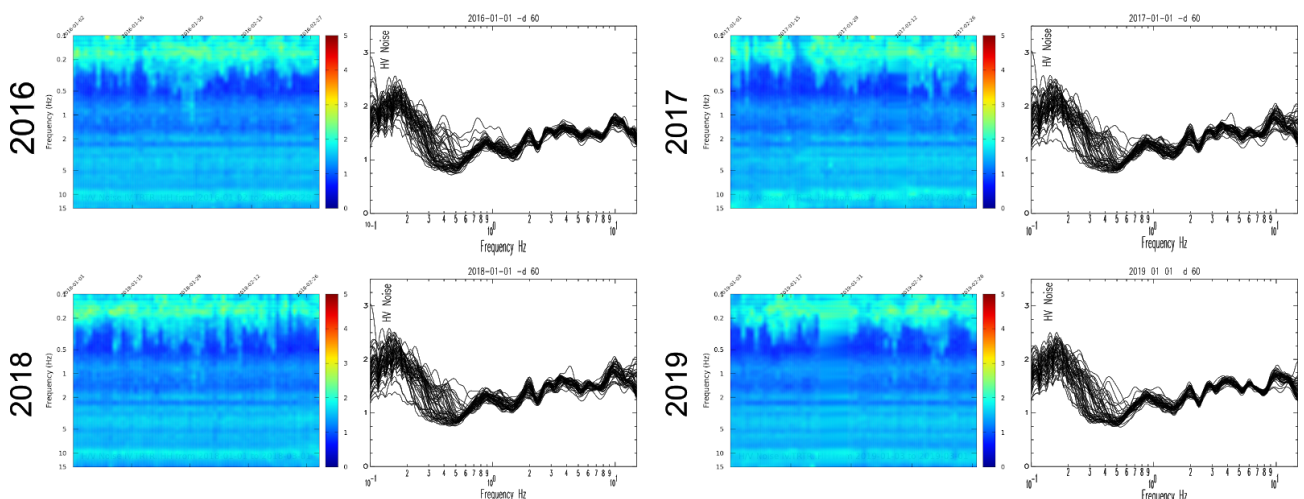


Figure 8. H/V spectral ratios using two months of continuous data extracted from IV.TRTR station starting from the 1st of January for the years 2016, 2017, 2018 and 2019. For each year, the continuous H/V curve is reported as contouring as a function of time on the left, with the color scale proportional to the amplitude of the H/V ratio. The daily average H/V curves are overlaid on the right panel.



2.3 Array analysis

The acquired data were processed using the *GEOPSY* software tools (www.geopsy.org) in order to extract the surface-wave dispersion properties of subsoil by applying frequency-wavenumber (FK) transform to the seismic signals. We analyzed using the FK technique the active data recorded by the linear array of geophones, and the passive data recorded by the seismic stations deployed in 2D configuration in Figure 3. Passive data recorded by the linear array of geophones were also processed by a cross-correlation technique.

2.3.1 Active data from the 1D array of geophones

The 72 vertical geophones were aligned in a straight line (yellow line in Fig. 3) and were equally spaced of 1 m. For the MASW analysis, we acquired the seismic signals produced by the impact of a 5 kg hammer on the ground. The shots were made along the line at distances (offset) of -5 m, -2, 35.5m, 73m and 76 m from the position of the first geophone (CH01 in Fig. 1 considered at 0m). In each shot point, the measurements were repeated three times in order to increase the signal-to-noise ratio. The seismic data were acquired using three multichannels systems (Geode manufactured by Geometrics) with a sampling rate of 0.125 ms for a duration of 2 s. Figure 4 illustrates the deployment of the MASW survey.

We also used the same linear array of 72 vertical geophones to acquire passive data, changing the sampling rate at 0.004 s (250 Hz) and recording several continuous records each of a time length of 4 minutes. The whole duration of passive data collected from the linear array of geophones was 1 hour and 40 minutes. Figure 9 shows the results obtained with the linear active survey (MASW). The analysis highlights a fairly consistent dispersion curve in the frequency range 6-50 Hz, with apparent phase-velocities between 150-350 m/s. Some small differences are observed between the shots at offset -5 and -2 m (from CH01) and the remaining shots, probably related to the presence of shallow soft colluvial deposits in the eastern sector of the MASW line (please refer to the geological map).



2.3.2 Passive data from the 1D array of geophones

The passive data recorded by geophones were analyzed in terms of cross-correlation (CC) using an ad hoc software (details in Vassallo et al. 2019). The cross-correlation functions are computed at the different geophones pair of the linear array, after one-bit normalization and spectral whitening (Bensen et al. 2007). To compute the dispersion curve of the seismic signals emerging from the cross-correlation functions, we applied a Constant Velocity Stack (CVS) analysis (Yilmaz, 1987). The cross-correlation functions were filtered in different frequency bands within 1-50 Hz, and for each band, the cross-correlation functions were shifted back in time according to the theoretical surface travel times computed for different constant velocities (from 50 m/s until 2000 m/s using a velocity step of 10 m/s). For each frequency band and applied velocity correction, the Phase-Weighted Stack (PWS, Schimmel and Paulsen, 1997) is computed, and the absolute maximum of PWS allows to estimate the presence of a horizontally aligned phase in the corrected seismic section.

Fig. 10 shows the computed cross-correlations functions (organized according to the distance between station pairs) and the results of the velocity analysis. The dispersion curve (black line) is identified on the basis of the maximum value of the stack function at each frequency.

2.3.3 Passive data from the 2D array of seismic stations

We used the passive data of the TB seismic stations in Figure 3 considered as a 2D array. We derived Rayleigh phase dispersion curves (Fig. 10) searching from the FK maxima in the wavenumber plane (k_x , k_y) using a three-components high-resolution beamforming (Wathelet et al. 2108). The results of the three-component analysis shows a Rayleigh-wave dispersion curve in the frequency range 3-5 Hz with apparent velocity between 250 and 500 m/s.

From the same analysis, it was not possible to estimate a Love-wave dispersion curve.

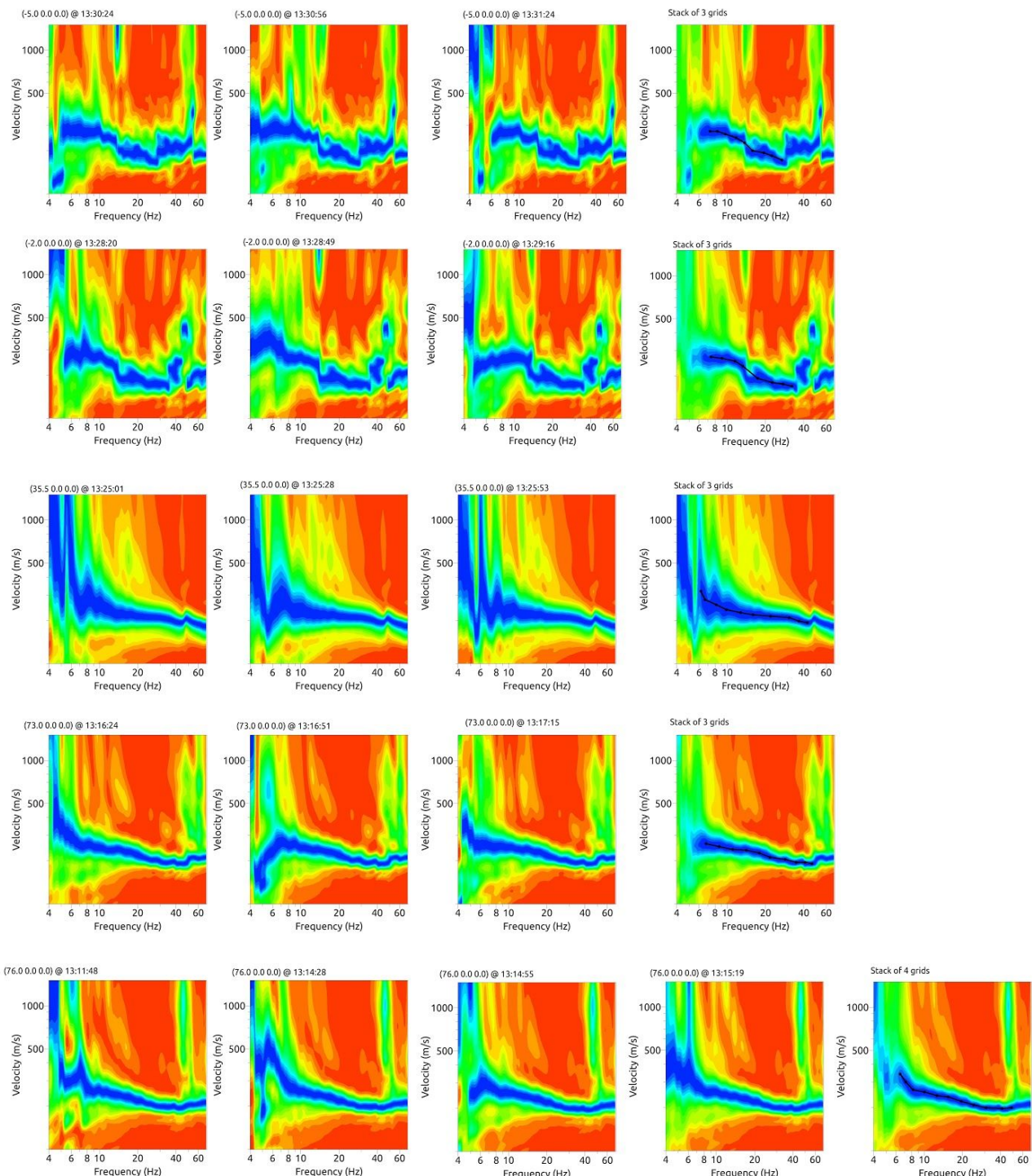


Figure 9. FK analysis on active data acquired by the MASW linear array of geophones. The results are shown for each shot; from top to down the offset is -5 m, -2 m, 35.5 m, 73m and 86m. Plots in the same horizontal panel refer to the same shot offset location. The plot of the last column shows the stack image obtained for the same offset; the black curve is the picked dispersion curve.

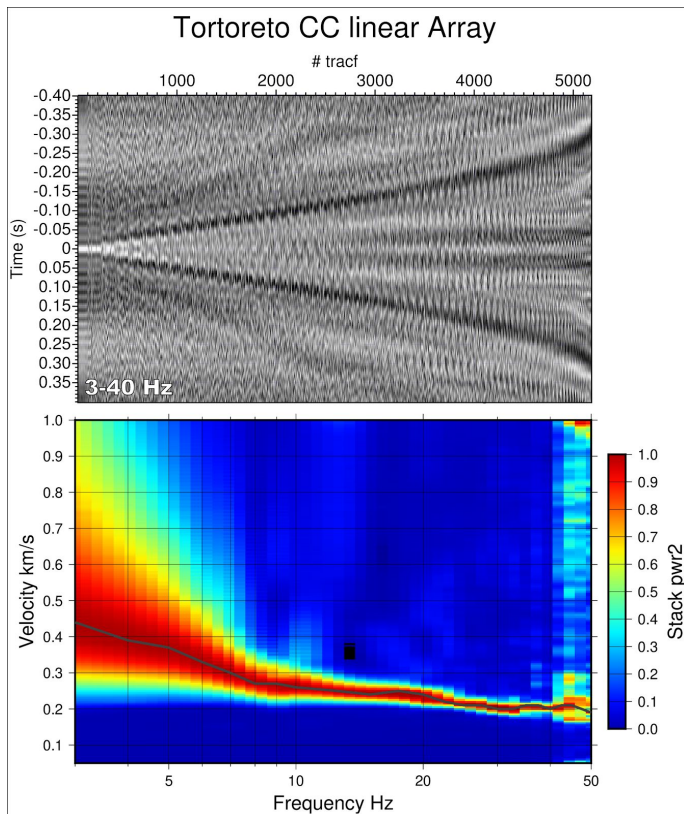


Figure 10. Cross-correlation (CC) analysis on passive data acquired by the 1D array of geophones. Top panel shows the CC signals estimated between 3-40 Hz. Bottom panel shows the resulting dispersion curve with the color scale proportion to the Phase-Weighted Stack (PWS); the black curve is the picked dispersion curve.

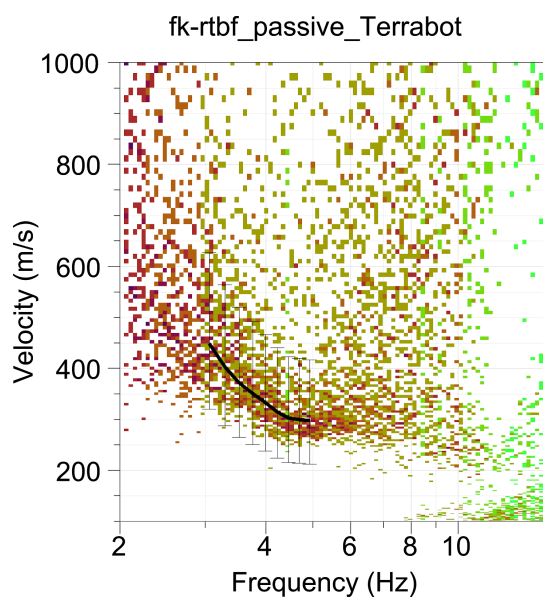


Figure 11. FK analysis on passive data acquired by the 2D array of Terrabot (see Fig. 3). The black curve is the picked dispersion curve.



2.3.4 Selection of the dispersion curve

For the selection of the final dispersion curve to be used in the inversion step, we combine all the experimental curves obtained in the previous analyses (summarized in Figs 9, 10, and 11) on active and passive data. The selected dispersions are reported in Fig. 12 showing a good agreement among the different techniques. An average dispersion was then computed (the black dashed curve) using the experimental curves (Fig. 12).

The final mean dispersion curve is in the frequency range 3-50 Hz, with apparent velocity values ranging from 450 m/s (at 3 Hz) up to 200 m/s (at 50 Hz). The maximum wavelength of our dispersion curve is 150 m , and as an experimental rule the depth of investigation is linked to $\frac{1}{2}$ or $\frac{1}{3}$ of the maximum wavelength (i.e. between 50-75 m of depth).

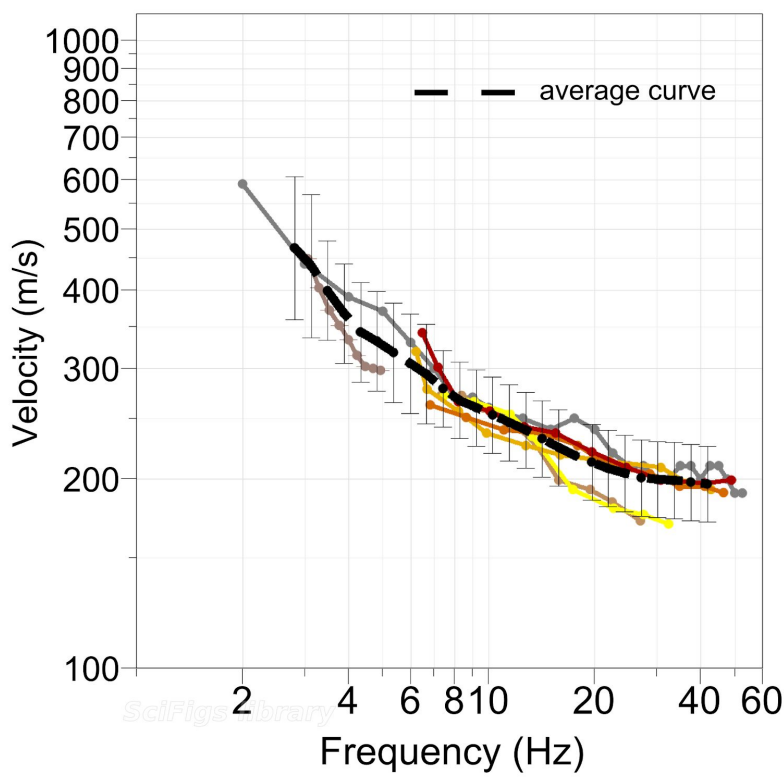


Figure 12. The final dispersion curve selected for the inversion step was computed as the average (black dashed curve) of the experimental curves (see Fig.s 9, 10 and 11). The experimental dispersions are the grey curve from 1D CC analysis on passive signals, the brown curve from 2D array analysis on passive data, the remaining curves (in red, magenta, orange and yellow color) are from active 1D analysis.

B3. 1D SEISMIC VELOCITY MODEL

The final dispersion curve used as target in the inversion procedure is the black one of Fig. 12. To proceed with the inversion step, the dispersion curve derived from the vertical component of motion has been associated with the fundamental mode of Rayleigh wave. Then, we inverted through the geopsy tool the apparent surface-wave dispersion curve for recovering the shear-wave velocity (V_s) model. Because in the frequency band 1-10 Hz the HV curves were with very low amplitude peaks (see Figs 7 and 8), they were not considered during the inversion step. However we note that these H/V peaks are well persistent in time.

The resulting velocity models after the inversion of the dispersion curve are shown in Fig. 13. We tested several simple starting model-parameterization composed of a few layers (uniform or with linear increase of velocity) over halfspace. Our best results show (Fig. 13) an uppermost layer with thickness around 15-20 m characterized by a linear increase of shear-wave velocity (V_s) from 200 m/s to 320-280 m/s, a second uniform layer at V_s of 320-380 m/s up to 40-50 deep, and then the bottom layer with V_s of 500-650 m/s. The best V_p and V_s models (i.e. lowest misfit) resulting from the inversion are shown in Fig. 14 and Table 1.

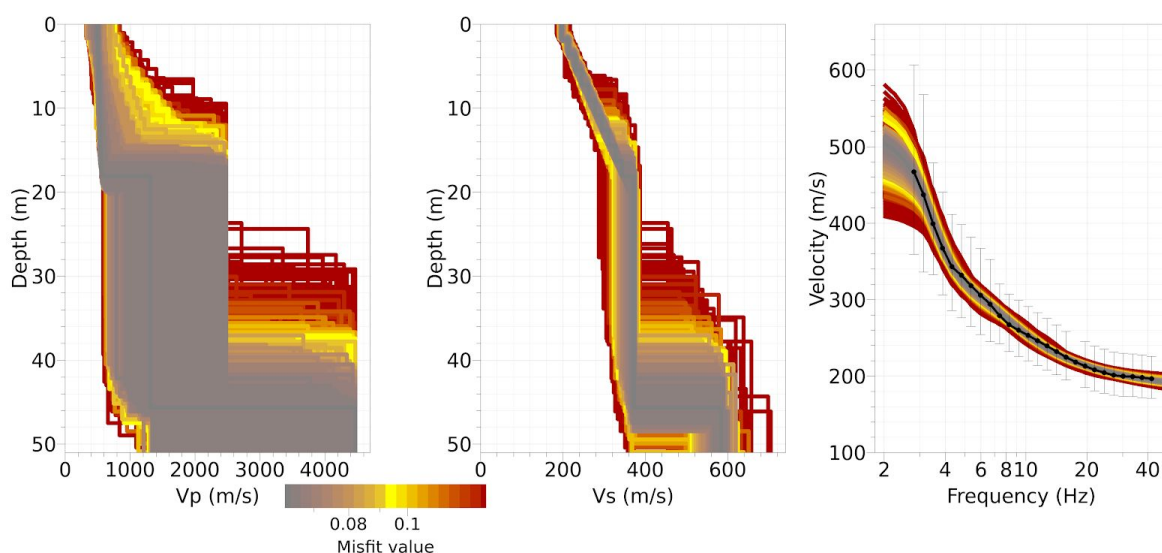


Figure 13. Resulting models after the inversion of the dispersion curves (the field dispersion is shown in black colour; the color scale is proportional to the misfit between experimental curve and theoretical models). The best V_p and V_s model (i.e. lowest misfit) are presented in Fig. 14.

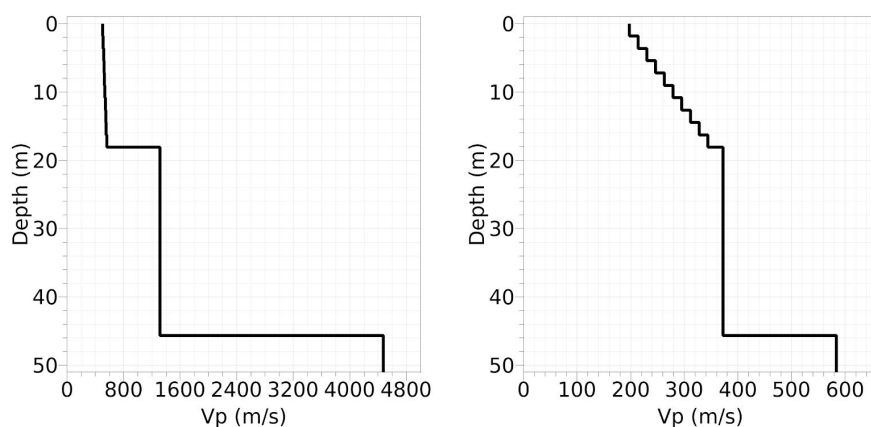


Figure 14. Best Vp and Vs models (extracted from the models of fig. 10) after the inversion of the apparent surface-wave Rayleigh dispersion curve.

Table 1. Best-fit model

| From (m) | To (m) | Thickness (m) | Vs (m/s) | Vp (m/s) |
|----------|--------|---------------|----------|----------|
| 0 | 1,81 | 1,81 | 197 | 503 |
| 1,81 | 3,62 | 1,81 | 213 | 509 |
| 3,62 | 5,43 | 1,81 | 230 | 516 |
| 5,43 | 7,24 | 1,81 | 246 | 522 |
| 7,24 | 9,05 | 1,81 | 262 | 529 |
| 9,05 | 10,86 | 1,81 | 279 | 535 |
| 10,86 | 12,67 | 1,81 | 295 | 542 |
| 12,67 | 14,48 | 1,81 | 311 | 548 |
| 14,48 | 16,29 | 1,81 | 327 | 555 |
| 16,29 | 18,1 | 1,81 | 344 | 561 |
| 18,1 | 45,66 | 27.56 | 372 | 1313 |
| 45,66 | 50 | 4.34 | 584 | 4473 |



B4. CONCLUSION

Surface-wave analysis at IV.TRTR station indicates a site of soil class C (Table 2). The best V_p and V_s models (i.e. lowest misfit) resulting from the inversion are proposed in Fig.s 13 and 14 and Table 1. HV noise spectral ratios of the temporary stations are characterized by a predominant peak at very low frequency (0.1-0.2 Hz) which could be tentatively related to a very deep (order of 1 km) seismic contrast or to the presence of the near Adriatic sea. Several peaks of very weak amplitude are also emerging in the frequency band 1-10 Hz. All the H/V peaks in the low- and high-frequency range are confirmed by the analysis of continuous two months data records extracted at the station IV.TRTR for different years (Fig. 8). Because of the low amplitude level of the H/V peaks within 1-10 Hz, we prefer to not indicate a resonance frequency in this report. The data analysis of the linear array of geophones and 2D array of stations gives a final dispersion curve from 3 to 50 Hz (Fig. 12), characterized by relatively low values of apparent phase-velocity.

The inversion procedure provides the V_s models of Fig.s 13 and 14 where the bottom layer is found at a depth of 46 m (Table 1). According to the geological model, the uppermost layer with thickness of about 20 m and V_s increasing with depth is interpreted as a colluvial layer, overlaying a deposit of stratified yellow sands (Q1b). Downward, the bottom layer at depth around 50 m is interpreted as the blue-grey clays deposit (Q1a)

The V_{s30} retrieved from the best inverted model is 297 m/s (Table 2), therefore IV.TRTR is classified following EC8 or NTC08 as soil class C also taking into account the geological observation described in the first part of the report.

Table 2. f₀ value, and soil class following NTC08 and NTC18.

| f ₀ (Hz) | Note |
|---------------------|---|
| | Not clearly identified; the main H/V peak is at very low frequency (0.1-0.2 Hz). The H/V peaks between 1-10 Hz are very weak although very persistent with time |

| V _{s30} (NTC08 or EC8) | Soil Class |
|---------------------------------|------------|
| 297 m/s | C |



REFERENCES

Bensen, G.D., Ritzwoller, M.H., Barmin, M.P., Levshin, A.L., Lin, F., Moschetti, M.P., Shapiro, N.M. and Yang, Y., (2007). Processing seismic ambient noise data to obtain reliable broad-band surface wave dispersion measurements. *Geophysical journal international*, 169(3), pp.1239-1260.

Carta Geologica-Tecnica per la Microzonazione Sismica di Livello 1, Regione Abruzzo, comune di Tortoreto(TE) (January, 2014)

Commissione Tecnica per la Microzonazione Sismica (2015). Microzonazione sismica. Standard di rappresentazione e archiviazione informatica, Versione 4.0b (Commissione tecnica inter-istituzionale per la MS nominata con DPCM 21 aprile 2011)

EC8. CEN (2004), Eurocode (EC) 8: Design of structures for earthquake resistance – Part 1 General rules, seismic actions and rules for buildings (EN 1998-1), Brussels

NTC08, 2008. Ministero delle infrastrutture e dei Trasporti (2008). Norme Tecniche per le Costruzioni (NTC08). Decreto Ministero Infrastrutture. GU Serie Generale n. 29 del 04-02-2008 - Suppl. Ordinario n. 30

NTC18, 2018. Ministero delle infrastrutture e dei Trasporti (2018). Norme Tecniche per le Costruzioni (NTC18). Decreto Ministero Infrastrutture. GU Serie Generale n. 42 del 20-02-2018 - Suppl. Ordinario n. 8

Schimmel, M. and Paulssen, H., (1997). Noise reduction and detection of weak, coherent signals through phase-weighted stacks. *Geophysical Journal International*, 130(2), pp.497-505.

Servizio Geologico d'Italia (1969). Geological Map of Italy (Sheet 133-134, Ascoli Piceno-Giulianova, scale 1:100.000). Istituto Poligrafico e Zecca dello Stato, Roma;

Vassallo, M., De Matteis, R., Bobbio, A., Di Giulio, G., Adinolfi, G.M., Cantore, L., Cogliano, R., Fodarella, A., Maresca, R., Pucillo, S. and Riccio, G. (2019). Seismic noise cross-correlation in the urban area of Benevento city (Southern Italy). *Geophysical Journal international*, 217(3), pp.1524-1542.

Wathelet, M., Guillier, B., Roux, P., Cornou, C. and Ohrnberger, M., (2018). Rayleigh wave three-component beamforming: signed ellipticity assessment from high-resolution frequency-wavenumber processing of ambient vibration arrays. *Geophysical Journal International*, 215(1), pp.507-523.



Wathelet M, Chatelain JL., Cornou C, Di Giulio G, Guillier B, Ohrnberger M, Savvaidis A (2020). Geopsy: A User-Friendly Open-Source Tool Set for Ambient Vibration Processing. Seismological Research Letters, 91(3), pp.1878-1889.

Yilmaz O. (1987). Seismic data processing in Investigations in Geophysics, 2: Soc. Expl. Geophys, series Eds., eds Doherty S.M., Neitzel E.B.

Servizio Geologico d'Italia (1969). Geological Map of Italy (Sheet 133-134, Ascoli Piceno, scale 1:100.000). Istituto Poligrafico e Zecca dello Stato, Roma;

Vezzani, L., & Ghisetti, F. (1998). Carta Geologica dell'Abruzzo, Scala 1:100.00, Regione Abruzzo, Settore Urbanistica-Beni ambientali e culturali, S.E.L.CA., Firenze;



Disclaimer and limits of use of information

The INGV, in accordance with the Article 2 of Decree Law 381/1999, carries out seismic and volcanic monitoring of the Italian national territory, providing for the organization of integrated national seismic network and the coordination of local and regional seismic networks as described in the agreement with the Department of Civil Protection.

INGV contributes, within the limits of its skills, to the evaluation of seismic and volcanic hazard in the Country, according to the mode agreed in the ten-year program between INGV and DPC February 2, 2012 (Prot. INGV 2052 of 27/2/2012), and to the activities planned as part of the National Civil Protection System. In particular, this document¹ has informative purposes concerning the observations and the data collected from the monitoring and observational networks managed by INGV.

INGV provides scientific information using the best scientific knowledge available at the time of the drafting of the documents produced; however, due to the complexity of natural phenomena in question, nothing can be blamed to INGV about the possible incompleteness and uncertainty of the reported data.

INGV is not responsible for any use, even partial, of the contents of this document by third parties and any damage caused to third parties resulting from its use.

The data contained in this document is the property of the INGV.

Esclusione di responsabilità e limiti di uso delle informazioni

L'INGV, in ottemperanza a quanto disposto dall'Art. 2 del D.L. 381/1999, svolge funzioni di sorveglianza sismica e vulcanica del territorio nazionale, provvedendo all'organizzazione della rete sismica nazionale integrata e al coordinamento delle reti sismiche regionali e locali in regime di convenzione con il Dipartimento della Protezione Civile.

L'INGV concorre, nei limiti delle proprie competenze inerenti la valutazione della Pericolosità sismica e vulcanica nel territorio nazionale e secondo le modalità concordate dall'Accordo di programma decennale stipulato tra lo stesso INGV e il DPC in data 2 febbraio 2012 (Prot. INGV 2052 del 27/2/2012), alle attività previste nell'ambito del Sistema Nazionale di Protezione Civile.

In particolare, questo documento¹ ha finalità informative circa le osservazioni e i dati acquisiti dalle Reti di monitoraggio e osservative gestite dall'INGV.

L'INGV fornisce informazioni scientifiche utilizzando le migliori conoscenze scientifiche disponibili al momento della stesura dei documenti prodotti; tuttavia, in conseguenza della complessità dei fenomeni naturali in oggetto, nulla può essere imputato all'INGV circa l'eventuale incompletezza ed incertezza dei dati riportati.

L'INGV non è responsabile dell'utilizzo, anche parziale, dei contenuti di questo documento da parte di terzi e di eventuali danni arrecati a terzi derivanti dal suo utilizzo.

La proprietà dei dati contenuti in questo documento è dell'INGV.



This document is licensed under License

Attribution – No derivatives 4.0 International (CC BY-ND 4.0)

¹This document is level 3 as defined in the "Principi della politica dei dati dell'INGV (D.P. n. 200 del 26.04.2016)"

RESONANCE FREQUENCY

fo +/- STD [Hz]

Quality index 1

| | | | | | | | | | | | | | | |
|--|---|----------------|-------------------------|------------------------------|--|---|----------------------|-------|--------------|-------------------------|----------------------------|---------------------------|----------------|--------------|
| Source | Earthquake | Ambient noise | | | | | | | | | | | | |
| Ambient noise <table border="1"> <tr> <td>Method</td> <td>H/V</td> <td>Ellipticity</td> <td>Other</td> </tr> <tr> <td>fo +/- std [Hz]</td> <td></td> <td></td> <td></td> </tr> <tr> <td>Experiment date [DD/MM/YY]</td> <td>Distance from station [m]</td> <td>Lat. [WGS84]</td> <td>Lat. [WGS84]</td> </tr> </table> | | | Method | H/V | Ellipticity | Other | fo +/- std [Hz] | | | | Experiment date [DD/MM/YY] | Distance from station [m] | Lat. [WGS84] | Lat. [WGS84] |
| Method | H/V | Ellipticity | Other | | | | | | | | | | | |
| fo +/- std [Hz] | | | | | | | | | | | | | | |
| Experiment date [DD/MM/YY] | Distance from station [m] | Lat. [WGS84] | Lat. [WGS84] | | | | | | | | | | | |
| Environment <table border="1"> <tr> <td>Weather conditions</td> <td>Sunny</td> <td>Windy</td> <td>Rain</td> </tr> <tr> <td>Soil-sensor coupling</td> <td>Earth</td> <td>Asphalt</td> <td>Artificial</td> </tr> <tr> <td>Urbanization</td> <td>None</td> <td>Dense</td> <td>Scattered</td> </tr> </table> | | | Weather conditions | Sunny | Windy | Rain | Soil-sensor coupling | Earth | Asphalt | Artificial | Urbanization | None | Dense | Scattered |
| Weather conditions | Sunny | Windy | Rain | | | | | | | | | | | |
| Soil-sensor coupling | Earth | Asphalt | Artificial | | | | | | | | | | | |
| Urbanization | None | Dense | Scattered | | | | | | | | | | | |
| Equipment <table border="1"> <tr> <td>Sensor</td> <td>Type [acc/vel]</td> <td>manufacturer</td> <td>cut-off frequency [Hz]</td> </tr> <tr> <td>Digitizer</td> <td>Type</td> <td>Manufacturer</td> <td>Sampling frequency [Hz]</td> </tr> <tr> <td>Measurement</td> <td>Number</td> <td colspan="2">Duration [min]</td> </tr> </table> | | | Sensor | Type [acc/vel] | manufacturer | cut-off frequency [Hz] | Digitizer | Type | Manufacturer | Sampling frequency [Hz] | Measurement | Number | Duration [min] | |
| Sensor | Type [acc/vel] | manufacturer | cut-off frequency [Hz] | | | | | | | | | | | |
| Digitizer | Type | Manufacturer | Sampling frequency [Hz] | | | | | | | | | | | |
| Measurement | Number | Duration [min] | | | | | | | | | | | | |
| Analysis <table border="1"> <tr> <td>Software</td> <td>Fo uncertainty estimate from</td> </tr> <tr> <td>Smoothing type (e.g. triangular, Konno-Ohmachi, ...)</td> <td>Fo from individual windows H/V curve width Manual picking</td> </tr> <tr> <td>Window length [s]</td> <td></td> </tr> </table> | | | Software | Fo uncertainty estimate from | Smoothing type (e.g. triangular, Konno-Ohmachi, ...) | Fo from individual windows H/V curve width Manual picking | Window length [s] | | | | | | | |
| Software | Fo uncertainty estimate from | | | | | | | | | | | | | |
| Smoothing type (e.g. triangular, Konno-Ohmachi, ...) | Fo from individual windows H/V curve width Manual picking | | | | | | | | | | | | | |
| Window length [s] | | | | | | | | | | | | | | |

| | | | | | | | | | | | | | | | | | | | | | | | | | | | | | |
|---|-----------------------|--------------------------|-----------------------------|-----------------------|--------------------------|---------------------|----------|-----------------|---------------------|-----|-----|-------------------|--------------|-------------|--|--|--|--|--|--|-------------------|--------------|--------------|--|--|--|--|--|--|
| Earthquake <table border="1"> <tr> <td>Method</td> <td>HVSR</td> <td>SSR</td> <td>GIT</td> <td>Other</td> </tr> <tr> <td>fo +/- std [Hz]</td> <td></td> <td></td> <td></td> <td></td> </tr> </table> | | | Method | HVSR | SSR | GIT | Other | fo +/- std [Hz] | | | | | | | | | | | | | | | | | | | | | |
| Method | HVSR | SSR | GIT | Other | | | | | | | | | | | | | | | | | | | | | | | | | |
| fo +/- std [Hz] | | | | | | | | | | | | | | | | | | | | | | | | | | | | | |
| <table border="1"> <tr> <td>Recording period [DD/MM/YY]</td> <td>Number of earthquakes</td> <td>Epicentral distance [km]</td> <td>Magnitude range</td> </tr> <tr> <td>from</td> <td>to</td> <td>from</td> <td>to</td> </tr> </table> | | | Recording period [DD/MM/YY] | Number of earthquakes | Epicentral distance [km] | Magnitude range | from | to | from | to | | | | | | | | | | | | | | | | | | | |
| Recording period [DD/MM/YY] | Number of earthquakes | Epicentral distance [km] | Magnitude range | | | | | | | | | | | | | | | | | | | | | | | | | | |
| from | to | from | to | | | | | | | | | | | | | | | | | | | | | | | | | | |
| HVSR <table border="1"> <tr> <td>Seismic phase</td> <td>P</td> <td>S</td> <td>Coda</td> <td>S + coda</td> <td>All</td> <td>window duration [s]</td> <td>Min</td> <td>Max</td> </tr> <tr> <td></td> <td></td> <td></td> <td></td> <td></td> <td></td> <td></td> <td></td> <td></td> </tr> </table> | | | Seismic phase | P | S | Coda | S + coda | All | window duration [s] | Min | Max | | | | | | | | | | | | | | | | | | |
| Seismic phase | P | S | Coda | S + coda | All | window duration [s] | Min | Max | | | | | | | | | | | | | | | | | | | | | |
| | | | | | | | | | | | | | | | | | | | | | | | | | | | | | |
| SSR <table border="1"> <tr> <td>Seismic phase</td> <td>P</td> <td>S</td> <td>Coda</td> <td>S + coda</td> <td>All</td> <td>window duration [s]</td> <td>Min</td> <td>Max</td> </tr> <tr> <td></td> <td></td> <td></td> <td></td> <td></td> <td></td> <td></td> <td></td> <td></td> </tr> <tr> <td>Reference station</td> <td>Lat. (WGS84)</td> <td>Lon. (WGS84)</td> <td></td> <td></td> <td></td> <td></td> <td></td> <td></td> </tr> </table> | | | Seismic phase | P | S | Coda | S + coda | All | window duration [s] | Min | Max | | | | | | | | | | Reference station | Lat. (WGS84) | Lon. (WGS84) | | | | | | |
| Seismic phase | P | S | Coda | S + coda | All | window duration [s] | Min | Max | | | | | | | | | | | | | | | | | | | | | |
| | | | | | | | | | | | | | | | | | | | | | | | | | | | | | |
| Reference station | Lat. (WGS84) | Lon. (WGS84) | | | | | | | | | | | | | | | | | | | | | | | | | | | |
| GIT <table border="1"> <tr> <td>Parameters</td> <td>Free (to be inverted)</td> <td>Imposed</td> </tr> <tr> <td></td> <td></td> <td></td> </tr> <tr> <td>Reference paper</td> <td></td> <td></td> </tr> <tr> <td>Reference station</td> <td>Lat. (WGS84)</td> <td>Lon (WGS84)</td> </tr> </table> | | | Parameters | Free (to be inverted) | Imposed | | | | Reference paper | | | Reference station | Lat. (WGS84) | Lon (WGS84) | | | | | | | | | | | | | | | |
| Parameters | Free (to be inverted) | Imposed | | | | | | | | | | | | | | | | | | | | | | | | | | | |
| | | | | | | | | | | | | | | | | | | | | | | | | | | | | | |
| Reference paper | | | | | | | | | | | | | | | | | | | | | | | | | | | | | |
| Reference station | Lat. (WGS84) | Lon (WGS84) | | | | | | | | | | | | | | | | | | | | | | | | | | | |

Vs30

Vs30 +/- STD [m/s]

Quality index 1

| | | | | | |
|--------|--------------------------|---------------------------|-------------------------------|---------|---------------|
| Source | Geophysical measurements | Geotechnical measurements | Digital Elevation Model (DEM) | Geology | DEM & Geology |
|--------|--------------------------|---------------------------|-------------------------------|---------|---------------|

Geophysical measurements

| Method | Surface waves methods (active, passive methods) | Borehole methods (DH, CH, PS-Logging) |
|------------------------|---|---------------------------------------|
| Vs30 +/- STD [m/s] | From Vs(z) | From Down-Hole |
| | | |
| | From Vr40 | From Cross-Hole |
| | | |
| | From Vs _z -Vs30 correlation | From PS Logging |
| | | |
| Reference relationship | | |
| | Vsz - Vs30 | |

Geotechnical measurements

| Method | N-SPT | CPT | Shear strength | OTHER |
|----------------------------|---------------------------|--------------|----------------|-------|
| Vs30 +/- STD [m/s] | | | | |
| Experiment date [DD/MM/YY] | Distance from station [m] | Lat. [WGS84] | Lon. [WGS84] | |

| | |
|-----------------------------|----------------|
| Reference relationship | N-SPT |
| Vs30-geotechnical parameter | CPT |
| | Shear strength |
| | Other |

Geology

| Method | Geological map | Stratigraphic log |
|------------------------|----------------------------|--------------------------------|
| Vs30 +/- STD [m/s] | | |
| Geological map scale | | |
| Geological unit name | | |
| Stratigraphic log | Experiment date [DD/MM/YY] | Lat. [WGS84] Lon. [WGS84] |
| Reference relationship | | |
| Vs30-geology | | |
| Reference relationship | | |
| Vs30-Stratigraphic log | | |

Digital Elevation Model

| | |
|------------------------|--|
| Vs30 +/- STD [m/s] | |
| DEM resolution | |
| Reference relationship | |
| Slope - Vs30 | |

| | |
|-------------|------|
| Slope range | from |
| | to |

DEM & GEOLOGY

| |
|---|
| Vs30 +/- STD [m/s] |
| Reference relationship Slope - Vs30 - geology |

Vs profile

Quality index 1

| Source | Non-invasive methods (active and/or passive seismics) | | Invasive methods (measurement in borehole) |
|-----------------------|---|--------------------------------------|--|
| Active surface waves | Refraction | Cross-hole / Down-hole | |
| Passive surface waves | Refection | Geotechnical methods (CPT, SPT, ...) | |
| HV / ellipticity | | PS-Logging | |

Non-invasive : surface waves methods

| Experiment date [DD/MM/YY] | Distance from station [m] | | Lat. [WGS84] center location | Lon. [WGS84] center location |
|----------------------------|---------------------------|-----|------------------------------|------------------------------|
| | Min | Max | | |

Active surface waves acquisition layout

| |
|------------------------------|
| Minimum receiver spacing (m) |
| Profile length (m)* |
| Geophones number |
| Number of profiles |

* Provide the length for the various profiles (e.g. 46 m, 94 m)

| |
|---------------------------------------|
| Geophone cut-off frequency (Hz) |
| Geophone type (vertical / horizontal) |
| Geophone manufacturer |
| Source (hammer, vibrator, ...) |
| Digitizer type |
| Digitizer manufacturer |

| | | | | | | | | | | | |
|--------------------|-------|-------|------|----------------------|-------|---------|------------|--------------|------|-------|-----------|
| Weather conditions | Sunny | Windy | Rain | Soil-sensor coupling | Earth | Asphalt | Artificial | Urbanization | None | Dense | Scattered |
|--------------------|-------|-------|------|----------------------|-------|---------|------------|--------------|------|-------|-----------|

Passive surface waves acquisition layout

| |
|------------------------|
| Number of sensors |
| Minimum array aperture |
| Maximum array aperture |
| Number of arrays |
| Minimum duration [min] |

| |
|-------------------------------------|
| Sensor cut-off frequency (Hz) |
| Sensor type (vertical / horizontal) |
| Sensor manufacturer |
| Digitizer type |
| Digitizer manufacturer |

| | | | | | | | | | | | |
|--------------------|-------|-------|------|----------------------|-------|---------|------------|--------------|------|-------|-----------|
| Weather conditions | Sunny | Windy | Rain | Soil-sensor coupling | Earth | Asphalt | Artificial | Urbanization | None | Dense | Scattered |
|--------------------|-------|-------|------|----------------------|-------|---------|------------|--------------|------|-------|-----------|

Type of dispersion and/or H/V estimates

| | |
|-----------------|--------------------------------------|
| Rayleigh DC | Reference paper (Name, Journal, DOI) |
| Love DC | |
| Ellipticity | |
| H/V (DFA, EHVR) | |
| H/V (SH) | |

Dispersion curves

| Rayleigh | Love |
|-----------------------|------|
| Min wavelength (m) | |
| Max. wavelength (m) | |
| Min. phase vel. (m/s) | |
| Max. phase vel. (m/s) | |
| Modes (R0, L0, ...) | |

H/V or Ellipticity curves

| | |
|---------------------|---------------------|
| Min. frequency (Hz) | Max. frequency (Hz) |
|---------------------|---------------------|

Inversion

| | | | | | |
|--|--------------------|--------------------|-------------------|--------------------------|---------------------|
| Rayleigh waves | Love waves | Ellipticity curves | H/V (DFA, EHVR) | H/V (SH) | resonance frequency |
| A priori information used in inversion | seismic refraction | | stratigraphic log | geotechnical information | water table depth |
| Inversion algorithm/code | | | | | |
| Reference | | | | | |

Non-invasive : body waves methods

| Experiment date [DD/MM/YY] | Distance from station [m] | | Lat. [WGS84] center location | Lon. [WGS84] center location |
|----------------------------|---------------------------|-----|---------------------------------|---------------------------------|
| | Min | Max | | |

Acquisition layout

| | |
|-------------------------------------|---------------------------------------|
| Receiver spacing (m) | Geophone cut-off frequency (Hz) |
| Profile length (m)* | Geophone type (vertical / horizontal) |
| Geophones number | Geophone manufacturer |
| Number of profiles | Source (hammer, vibrator, ...) |
| Shot spacing (m) - reflection meas. | Digitizer type |
| | Digitizer manufacturer |

* Provide the length for the various profiles (e.g. 46 m, 94 m)

| | | | | | | | | | | | |
|--------------------|-------|-------|------|----------------------|-------|---------|------------|--------------|------|-------|-----------|
| Weather conditions | Sunny | Windy | Rain | Soil-sensor coupling | Earth | Asphalt | Artificial | Urbanization | None | Dense | Scattered |
|--------------------|-------|-------|------|----------------------|-------|---------|------------|--------------|------|-------|-----------|

Processing methods

| | |
|-----------------------|--------------------------------------|
| | Reference paper (Name, Journal, DOI) |
| classical refraction | |
| refraction tomography | |
| classical reflection | |
| advanced method | |

Invasive methods

OTHER

| Down-Hole | Cross-Hole | PS-Logging | SPT | CPT |
|---------------------------|------------|------------|-----|-----|
| Borehole depth (m) | | | | |
| Geophone type | | | | |
| Source type | | | | |
| Distance between wells | | | | |
| Depth resolution (m) | | | | |
| Latitude (WGS84) | | | | |
| Longitude (WGS84) | | | | |
| Distance from station (m) | | | | |
| P-wave velocity | | | | |
| S-wave velocity | | | | |

Processing methods

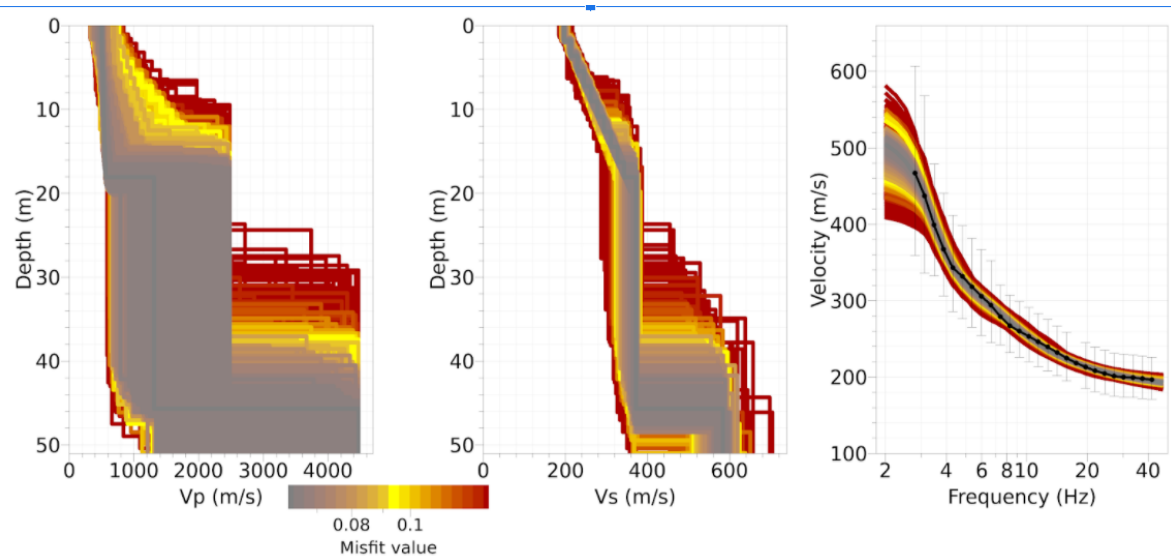
| | |
|------------|---|
| | Reference paper (Name, Journal, DOI) or ASTM norm |
| Down-Hole | |
| Cross-Hole | |
| PS-Logging | |
| SPT | |
| CPT | |
| OTHER | |

Authoritative velocity profile

Note: You do not have to fill in all the columns. You can provide either single values for Vp or Vs (e.g. profiles derived from borehole measurements) or either a range for Vp and Vs (e.g. profiles derived from stochastic surface waves inversion)

| Is Vs derived from Vp ? | | Yes | No | Vs range | | Vp range | | | |
|-------------------------|---------------------|----------|-----------------|----------|-----------------|-----------------|-----------------|-----------------|-----------------|
| Top depth (m) | Bottom depth (m) | Vp (m/s) | STD Vp (m/s) | Vs (m/s) | STD Vs (m/s) | Vs min (m/s) | Vs max (m/s) | Vp min (m/s) | Vp max (m/s) |
| | | | | | | | | | |

Figure with authoritative velocity profiles



Surface geology

Quality index 1

| | |
|--------|---|
| Source | Cartography (geological, lithological, ...) |
|--------|---|

| |
|--------------|
| Field survey |
|--------------|

| |
|-------------------|
| Stratigraphic log |
|-------------------|

Geological map

| | |
|--------------------------------------|--|
| Map reference | |
| Map scale | |
| Map sheet | |
| Predominant geologic/lithologic unit | Name : Description : Age : Thickness : Rock mass structure : |
| Fault presence | |
| Weathering | |
| Cross-section | |

Field survey

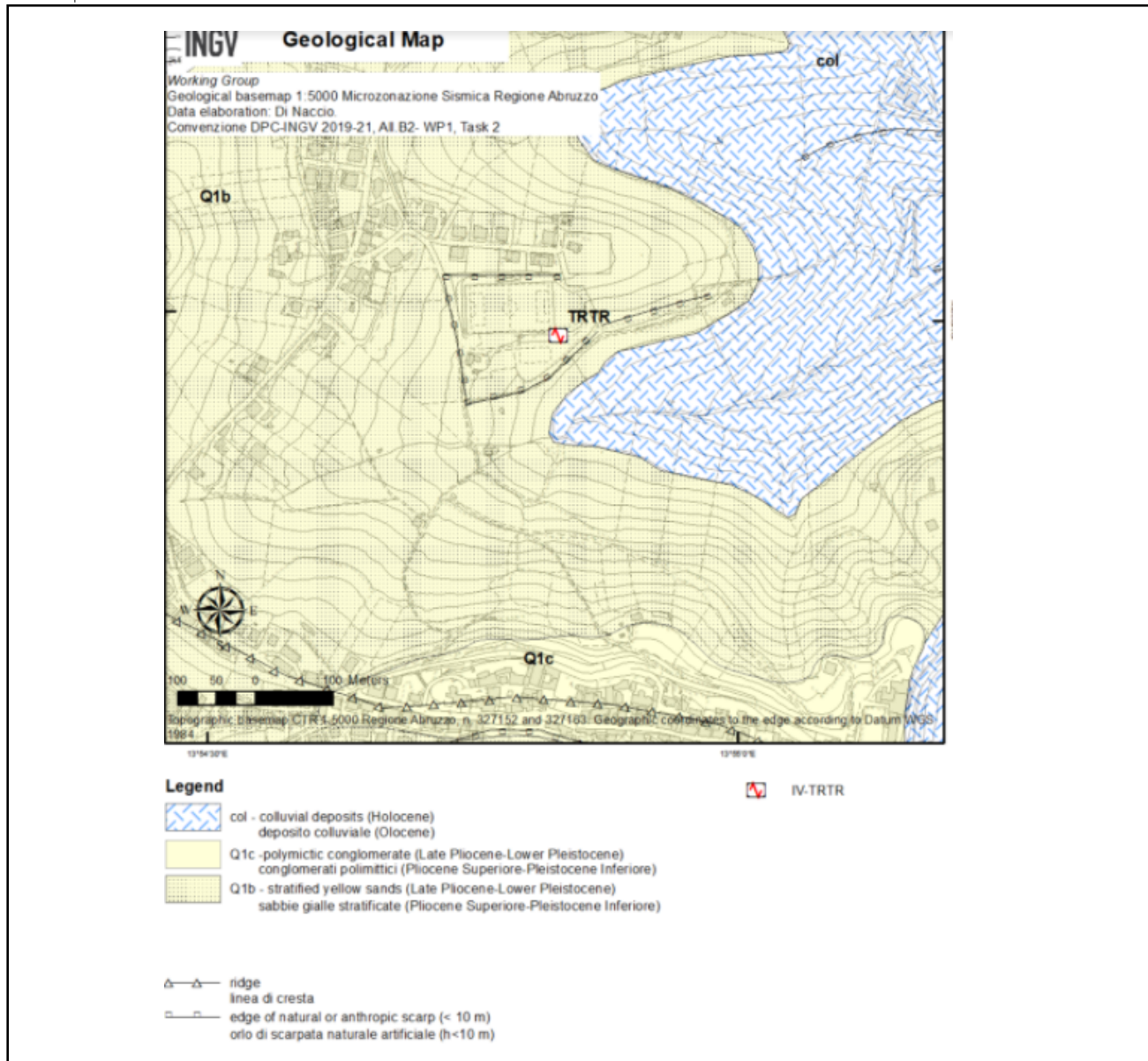
| | |
|--------------------------------------|--|
| Map reference | |
| Map scale | |
| Predominant geologic/lithologic unit | Name : Description : Age : Thickness : Rock mass structure : |
| Fault presence | |
| Weathering | |
| Cross-section | |

Stratigraphic log

| | | |
|---------------|------------------|---------------------------|
| log depth (m) | | |
| Top depth (m) | Bottom depth (m) | Stratigraphic description |

Surface geology

Map



Site class

Site class

Quality index 1

Reference building code for site classification
(EC8-1, EC8-2, NEHRP, national code, ...)

Source

Geophysical measurements

Geotechnical measurements

Digital Elevation Model (DEM)

Geology

DEM & Geology

Reference relationship geology - soil class

Reference relationship slope from DEM - soil class

Reference relationship slope from DEM - geology - soil class

Parameters for deriving soil class as prescribed in building code

Seismological bedrock depth

Depth +/- STD [m]

Quality index 1

| | |
|--------|---------------------|
| Source | Vs profiles |
| | Resonance frequency |

| |
|-------------------|
| Geology |
| Stratigraphic log |

Other (gravity, seismic refraction, TDEM, ...)

Vs profile

| | Non-invasive methods | Invasive seismic methods | Geotechnical methods |
|--------------------------|----------------------|--------------------------|----------------------|
| Bedrock depth +/- STD(m) | | | |
| Bedrock Vs +/- STD(m) | | | |
| Bedrock Vp +/- STD(m) | | | |
| Is Vs derived from Vp ? | Yes | No | |

Resonance frequency

| |
|---|
| Bedrock depth +/- STD(m) |
| Reference relationship Fo - bedrock depth |
| |

Geology

| |
|--------------------------|
| Bedrock depth +/- STD(m) |
| Bedrock geological unit |
| Reference |

Stratigraphic log

| |
|--------------------------|
| Bedrock depth +/- STD(m) |
| Bedrock geological unit |
| Reference |

Other methods

| Bedrock depth +/- STD(m) | Reference |
|--------------------------|-----------|
| Gravity | |
| Seismic refraction | |
| Seismic reflection | |
| TDEM | |

Engineering bedrock depth

Depth +/- STD [m]

Quality index 1

Reference Vs related to engineering bedrock in m/s

Reference building code for site classification (EC8-1, EC8-2, NEHRP, national code, ...)

Source

Vs profile

Geology

Stratigraphic log

Vs profile

Non-invasive methods

Invasive seismic methods

Geotechnical methods

Bedrock depth +/- STD(m)

Is Vs derived from Vp ?

Yes

No

Geology

Bedrock depth +/- STD(m)

Bedrock geological unit

Reference

Stratigraphic log

Bedrock depth +/- STD(m)

Bedrock geological unit

Reference